

Watching a metal collapse: Examining cerium's $\gamma \leftrightarrow \alpha$ transformation using X-ray diffraction of compressed single and polycrystals

K.T. Moore^{a,*}, L. Belhadi^b, F. Decremps^b, D.L. Farber^a, J.A. Bradley^a, F. Ocelli^c,
M. Gauthier^b, A. Polian^b, C.M. Aracne-Ruddle^a

^a Lawrence Livermore National Laboratory, Livermore, CA 94550, USA

^b IMPMC – Université Pierre et Marie Curie – UPMC, 75252 Paris Cedex 05, France

^c CEA, DAM, DIF, F-91297 Arpajon, France

Received 26 January 2011; received in revised form 3 June 2011; accepted 6 June 2011

Available online 29 June 2011

Abstract

Numerous investigations have been performed on Ce metal since the discovery of the $\gamma \rightarrow \alpha$ phase transformation, where a face-centered cubic structure is believed to collapse isostructurally with a volume change of $\sim 17\%$. However, two questions have yet to be answered definitively. First, is the transformation truly isostructural or is the face-centered cubic structure lost in α -Ce due to symmetry breaking? Second, if the transformation is isostructural does the face-centered cubic structure stay in crystallographic orientation through the volume collapse? Here, we use high-pressure and high-temperature X-ray diffraction measurements to examine single and polycrystalline samples of Ce in the vicinity of the $\gamma \leftrightarrow \alpha$ transformation. This was achieved by successive continuous compression and decompression in a diamond anvil cell at temperatures under, at and above the critical point. Our results show that the crystal structure remains face-centered cubic for both the γ and α phases. The results also show that the face-centered cubic structure retains its crystallographic orientation, simply reducing in volume during the $\gamma \rightarrow \alpha$ phase transformation. Upon transformation to α , polycrystalline samples show increased diffraction peak broadening, while single crystals show increased streaking. These changes in diffraction can be attributed to increased damage and lattice misorientation from the transformation. Using a simple atomic lattice model, we show that a periodic array of misfit edge dislocation is necessary to accommodate the large volume difference at the γ - α interface and this could act as a source of the edge dislocations needed to produced previously observed deformation bands.

Published by Elsevier Ltd. on behalf of Acta Materialia Inc.

Keywords: Cerium; Rare earth; Phase transformation; X-ray diffraction; High pressure

1. Introduction

Cerium is a fascinating metal. Under atmospheric pressure, it exhibits four solid allotropic crystal structures between absolute zero and melting at 1071 K. These are designated in Fig. 1 as α , which is face-centered cubic (fcc); β , which is double hexagonal close packed (dhcp); γ , which is also fcc; and δ , which is body-centered cubic (bcc). There are large hystereses between the transformations of α , β

and γ , causing phase boundaries to be kinetic approximations. Often mixtures of two or even three phases have been observed to persist metastably in single-phase fields [1,2]. The γ - α phase boundary terminates in a critical point at 1.5 ± 0.1 GPa and 480 ± 10 K [3], making Ce the only metallic element known to exhibit a critical point. During the $\gamma \rightarrow \alpha$ transformation, Ce is believed to isostructurally transform from a larger fcc structure to a smaller fcc structure. Put simply, the fcc unit cell collapses from the γ phase to α with applied pressure and/or reduced temperature. The volume collapse can be as large as $\sim 17\%$ near the β phase field, but diminishes to zero near the critical point.

* Corresponding author. Tel.: +1 925 422 9741; fax: +1 925 422 6892.

E-mail address: moore78@llnl.gov (K.T. Moore).

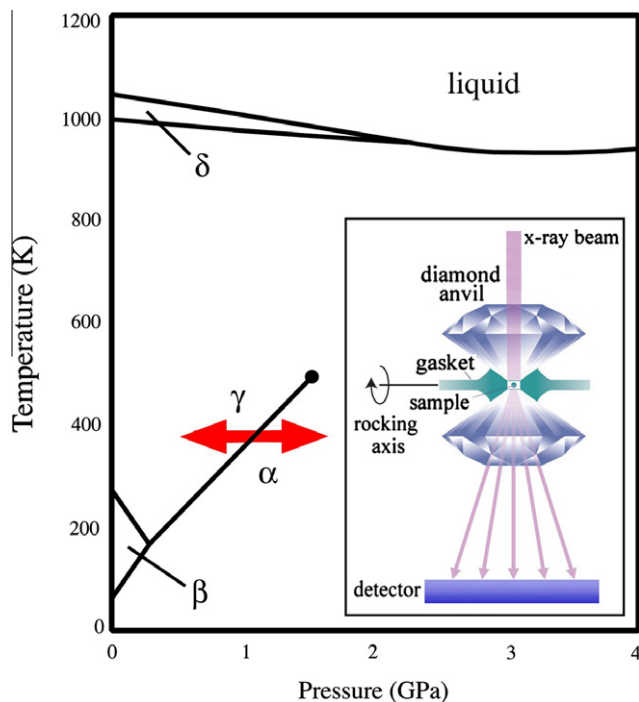


Fig. 1. Pressure–temperature phase diagram of Ce metal. The horizontal arrow shows an isothermal pressure path used to transform γ - to α -Ce in a DAC. (Inset) Experimental geometry of the DAC and X-ray beam.

Several interpretations of why this volume collapse occurs have been postulated. First was the promotion model, where a localized $4f$ electron is promoted to a pre-existent (spd) band of delocalized electrons [4]. Another was a Mott transition, where the localized $4f$ electrons on each atomic site merge with each other to create a delocalized $4f$ band of electrons [5]. A third was the Kondo volume-collapse model, where the $4f$ electrons mix quantum mechanically with the delocalized (spd) band, existing simultaneously as an atomic-like electron and in a large delocalized state [6].

The promotional model was challenged when Gustafson et al. [7] showed there was no significant change in the number of f electrons between α - and γ -Ce via positron lifetime and angular correlation measurements. The promotional model was further questioned by Compton scattering data [8] and X-ray absorption measurements of the L edges [9], which showed no substantial change in valence between α - and γ -Ce. The Mott transition theory was questioned by photoemission experiments that show the f level is located below the Fermi energy in both phases [10]. Magnetic form factor [11] and phonon density of states [12] measurements also disagree with a Mott transition, showing that the magnetic moment remains localized in both phases. Dynamical mean-field theory calculations of the optical properties of α - and γ -Ce [13] are in agreement with the optical data of van der Eb et al. [14], which gives support for the Kondo picture. However, the answer is not yet clear. Even with all three models available and an appreciable amount of theoretical attention, the issue

remains unresolved. In fact, there are even theoretical results supporting a combination of all three effects [15,16]. One key concept that is widely accepted, regardless of model, is that hybridization between $4f$ and valence electrons plays an integral role in the phase transformation, and experiments have clearly shown this occurs [17,18].

Electronic-structure driving forces aside, the behavior of a Ce crystal during the $\gamma \leftrightarrow \alpha$ phase transformation is of great interest. Reviewing experimental investigations of the transformation, it is clear that questions remain. First, is the $\gamma \leftrightarrow \alpha$ transformation truly isostructural? While the theoretical models above [4–16] assume an fcc–fcc transformation, Eliashberg and Capellmann [19] proposed that γ - and α -Ce are different phases separated by a boundary ending with a tricritical point. The experimental basis for their hypothesis was found in early X-ray diffraction work by Davis and Adams [20], where the compressibility was observed to diverge in the vicinity of the (tri)critical point for only the α phase. In such a case, the Landau theory of phase transformation imposes the symmetries of γ and α must be different, with a second-order phase transition beyond the terminal point. The fcc–fcc transformation was further questioned by Nikolaev and Michel though time-differential perturbed angular correlations measurements [21]. They postulate that γ -Ce is $Fm\bar{3}m$ and α -Ce is $Pa\bar{3}$, where the atomic point lattice remains fcc, but the symmetry is broken via electronic charge density [22]. Interestingly, an fcc to distorted fcc transition has been observed to occur in La [23] and Pr [24], the elements on either side of Ce in the periodic table, as well as in cerium-based alloys [25] and δ -Pu [26].

The second question is a logical progression of the first. If the γ and α phases are both fcc, does the structure retain crystallographic orientation through the transformation? In other words, does the fcc unit cell simply compress while keeping its crystallographic planes and directions? Or is there some rotation in the spirit of the Bain path that traces the energy of a bcc crystal as it is strained along the $\langle 001 \rangle$ axis until it becomes an fcc crystal? This is a fascinating question given that the volume change can be as high as $\sim 17\%$ during the $\gamma \leftrightarrow \alpha$ transformation. How the lattice will evolve and accommodate the immense strains of such a transformation has important and novel metallurgical implications.

Here, we present results from a series of high-pressure, high-temperature experiments formulated to answering these questions. Using a diamond anvil cell (DAC) and in situ resistive heating, we examine the $\gamma \leftrightarrow \alpha$ transformation in both single crystal and polycrystalline Ce metal using synchrotron-radiation X-ray diffraction. Our results show that the fcc structure is retained in both the α and γ phases, and that the crystal does in fact stay in orientation, simply reducing unit cell size during the $\gamma \rightarrow \alpha$ phase transformation. There is, however, increased damage and lattice misorientation concomitant with the transformation, which is evidenced by diffraction peak broadening and streaking, respectively. Using our data and a simple

atomic lattice model, we show that a periodic array of misfit edge dislocation is necessary to accommodate the large volume difference at the γ - α interface. The large misfit could act as a source of the edge dislocations needed to produce the previously observed deformation bands [27]. The results reported here are a detailed extension of our earlier work on the $\gamma \leftrightarrow \alpha$ transformation in Ce metal [28].

2. Experimental procedures

High-purity Ce samples were used in all experiments, since the physical properties of the metal are known to be affected by impurities even in small concentration. Polycrystalline samples were produced in a purpose-built crucible using a triarc furnace under an argon atmosphere starting from material scraped from a 99.99% cerium ingot using a diamond file in a dry nitrogen glove box. Single-crystal samples were prepared from an ingot grown at the Ames Laboratory, which was used in the historical first inelastic neutron scattering experiment of γ -Ce [29,30]. Crystals 60–80 μm in diameter and 20 μm in thickness were prepared by femtosecond laser cutting and mechano-chemical polishing techniques under controlled atmosphere [31]. A single-crystal with a $[0\ 0\ 1]$ surface normal was prepared for pressure experiments, ensuring a known orientation.

Helium was used as pressure-transmitting medium for DAC experiments. The sample and He were loaded within two diamonds with 800 μm culets and a 400 μm diameter rhenium gasket. Sample heating was achieved in the DAC with resistive heating, which enabled independent control of pressure and temperature without bringing the cell back to ambient conditions. The temperature was regulated using an electronic module and two K-type thermocouples, one glued to each anvil, yielding a measured accuracy better than 1 K. Hysteresis was determined through the measurement of the lattice parameter at constant temperature during compression and decompression at the rate of 0.04 bar min^{-1} on the membrane DAC. The pressure inside the cell was determined indirectly by fluorescence measurements of $\text{SrBO}_4:\text{Sm}^{2+}$ with an absolute uncertainty of about 10^{-2} GPa. Identical values of pressure were always determined before and after collection of each diffraction measurement.

Angle-dispersive X-ray diffraction measurements were performed at the ID09A beamline of the European Synchrotron Radiation Facility, using a monochromatic beam ($\lambda = 0.413818$ Å) focused to less than 5 μm full-width half-maximum. Sample-to-detector distance and detector tilt were calibrated using a Si standard and FIT2D software. Single crystal diffraction patterns were collected during a rotation of the sample between -20° and $+20^\circ$ about a vertical axis perpendicular to the beam axis, as shown in Fig. 1 inset.

Transmission electron microscopy (TEM) was performed on a polycrystalline Ce sample of 99.9% purity that was prepared and examined as described elsewhere [32,33].

3. Results

3.1. Polycrystalline metal

Polycrystalline samples were examined during compression at 334, 351, 374, 396, 423, 460 and 503 K, ensuring the $\gamma \leftrightarrow \alpha$ phase transformation was examined from near the β phase field to beyond the critical point. At each temperature, the sample was compressed and released while the crystal structure was monitored via X-ray diffraction. Data collected for an isothermal compression at 334 K are shown in Fig. 2, where the inset displays polycrystalline diffraction patterns for 0.44, 0.51, 0.57, 0.67 and 1.04 GPa. At 0.44 GPa the diffraction pattern shows peaks for only the γ phase, while at 1.04 GPa there are peaks for only α . Between these pressures there is a mixture of γ and α , which is illustrated in the main panel of Fig. 2 by the ratio of Bragg intensities ($[3\ 1\ 1]_\gamma$ to $[2\ 0\ 0]_\alpha$) as a function of pressure. The mixture of γ and α persists between 0.47 and 0.67 GPa, demonstrating the transformation hysteresis noted above [1,2].

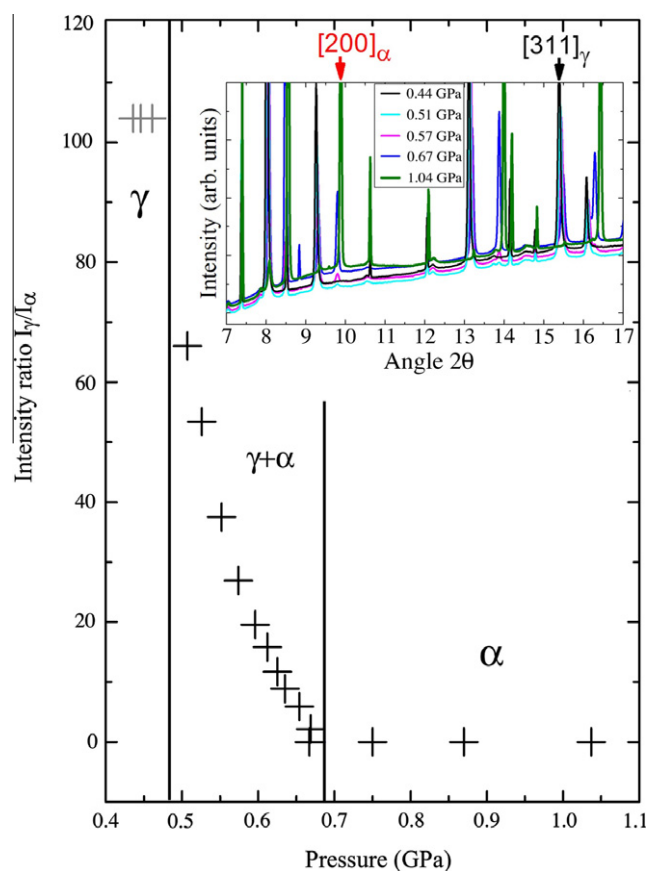


Fig. 2. A plot of the intensity ratio between the $[3\ 1\ 1]_\gamma$ and $[2\ 0\ 0]_\alpha$ reflections as a function of pressure, recorded during decompression of polycrystalline Ce metal. Below ~ 0.47 GPa there is only γ phase, between 0.47 and 0.67 GPa there is a mixture of γ and α , and above ~ 0.67 GPa there is only α phase. (Inset) Polycrystalline diffraction patterns for 0.44, 0.51, 0.57, 0.67 and 1.04 GPa.

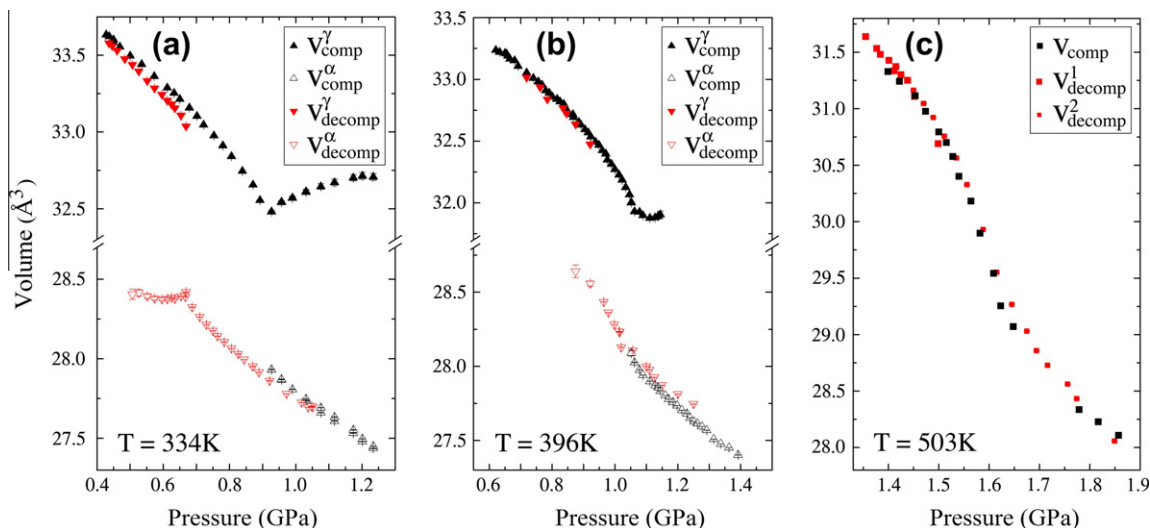


Fig. 3. Three pressure–volume plots showing the EOS of polycrystalline Ce metal: (a) $T = 334$ K, (b) $T = 396$ K and (c) $T = 503$ K. The EOS for 334 and 396 K both show hysteresis and coexistence zones of γ and α ; however, the EOS for 503 K changes smoothly and continuously with pressure. Since there is no clear designation between γ and α at 503 K, the data are plotted using red and black squares for a single fcc phase. (For interpretation of the references to colour in this figure legend, the reader is referred to the web version of this article.)

The equation-of-state (EOS) can be monitored at each temperature using X-ray diffraction. Three sets of data are shown in Fig. 3, where (a) is for 334 K, (b) is for 396 K and (c) is for 503 K. Results are plotted for both compression and decompression, since two sets of measurements ensure consistency of the transformation due to hysteresis. Fig. 3a plots the EOS of γ and α during compression, V_{comp}^{γ} and V_{comp}^{α} , respectively, and during decompression, $V_{\text{decomp}}^{\gamma}$ and $V_{\text{decomp}}^{\alpha}$, respectively. The data taken at 334 K show hysteresis and a mixture of γ and α during compression and release. The compression data (black triangles) show that the unit cell volume of γ decreases with increased pressure up to ~ 0.9 GPa, where α begins to form. Above this pressure the volume of γ increases until ~ 1.15 GPa, where it saturates, then collapses to α . During decompression a similar, but opposite behavior is observed: the unit cell of α increases until γ forms, then decreases for a short pressure interval until it increases again briefly and disappears.

The EOS for an isothermal compression recorded at 396 K shows similar trends although to a lesser extent. There is again hysteresis and a mixture of phases. There is also an increase in the volume of γ during compression once the α phase forms. However, during decompression α transforms to γ with no evidence of a reduction in the α volume.

The EOSs in Fig. 3a and b both show hysteresis and coexistence zones of γ and α . This behavior is observed up to 460 K, at which temperature the critical point is neared and the EOS begins to exhibit a smooth and continuous volume change. This is illustrated in Fig. 3c, which is an isothermal compression recorded at 503 K. Since there is no clear designation between γ and α at this temperature, we now switch to red and black squares for a single fcc phase. The data for compression are given as black

squares, V_{comp} , and the data for two separate decompressions are given as large and small red squares, V_{decomp}^1 and V_{decomp}^2 , respectively. In this data set, the EOS smoothly and continuously changes with pressure with no jump in volume.

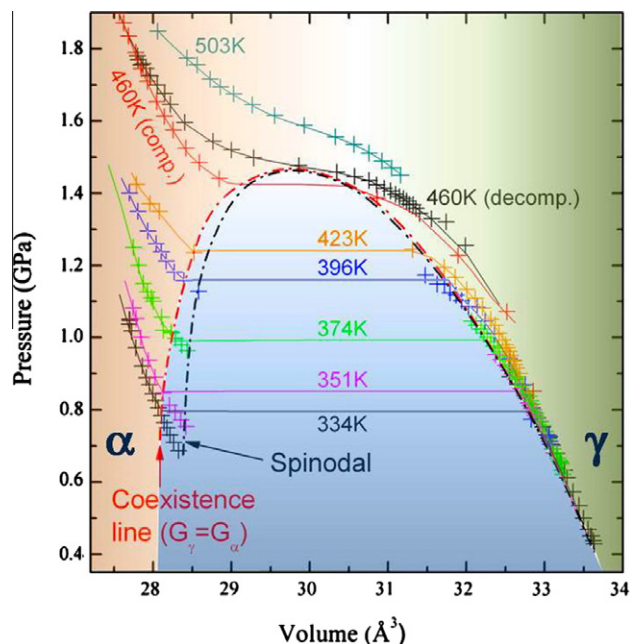


Fig. 4. Clapeyron diagram of polycrystalline Ce metal for several isotherms (neglecting kinetics effects in the coexistence regions). Above $T = 460$ K, the volume jump at the transition is no longer observed, replaced by a continuous variation with pressure. The coexistence (dotted red) line delimits the region where the system stands in a biphasic configuration, whereas the spinodal line (dashed–dotted black line) represents the boundary between metastable and unstable conditions. (For interpretation of the references to colour in this figure legend, the reader is referred to the web version of this article.)

The EOS for each isothermal compression can be plotted together, yielding the pressure–volume diagram shown in Fig. 4. From the plot it is apparent that a spinodal region forms, which is designated by the dark blue dash-dot line. The term “spinodal” is more commonly used in the context of a chemical spinodal [34–36], where a miscibility gap in temperature–chemistry space results in the spontaneous decomposition of a single crystal into two crystals with the same structure, but different compositions. The underlying driving force for this type of decomposition is a lowering of the Gibbs free energy (G). When formulating the equations for chemical spinodal decomposition [34], pressure is neglected (assumed one atmosphere) because we view metals as mostly incompressible, and for many examples this assumption is justified. However, the free energy of a solid is a function of pressure. Compressing a material to 10 GPa equates to an energy change of approximately $100 \text{ meV } \text{Å}^{-3}$. There are metals, such as Ce, where small amounts of pressure can change the electronic structure enough to drive phase transformations.

At temperatures greater than 460 K (see Fig. 4), there is a continuous EOS, where the fcc structure smoothly reduces in size with compression. However, below 460 K a region of immiscibility occurs in pressure–volume (P – V) space where two fcc crystals form, one with a small volume (α) and one with a large volume (γ). Typical of chemical spinodals, the P – V spinodal in Fig. 4 broadens with decreasing temperature (and pressure). The diagram clearly

illuminates the behavior of the $\gamma \leftrightarrow \alpha$ phase transformation with respect to pressure, temperature and volume.

The width of diffraction peaks was examined during the $\gamma \leftrightarrow \alpha$ transformation in hopes of gaining information on the quality of the crystal. The full width at half maximum (FWHM) of the [2 2 0] Bragg peak was recorded at various pressures and fit through calculated refinements. The results are shown in Fig. 5, where (a) is an isothermal compression at 374 K and (b) is one at 503 K. For both temperatures, the FWHM of the [2 2 0] Bragg peak and the volume are plotted as a function of pressure. In Fig. 5a, the EOS during compression for γ and α are given as before, with V_{comp}^{γ} and V_{comp}^{α} , respectively. The FWHM of the [2 2 0] diffraction peak during compression for γ and α are given as W_{comp}^{γ} and W_{comp}^{α} , respectively. Examining the EOS in Fig. 5a, which is marked by the solid red and black triangles, the $\gamma \leftrightarrow \alpha$ transformation is apparent. The FWHM of the [2 2 0] diffraction peak for γ increases near the transformation until it ends due to the presence of pure α -Ce. The [2 2 0] peak for α is slightly broader than for γ before the transformation.

The EOS for 503 K in Fig. 5b is given only by V_{comp} , since there is one fcc phase that continuously changes with pressure. Similarly, the FWHM is given only by W_{comp} . A maximum occurs in the width of the [2 2 0] diffraction peak near the inflexion point of the EOS, then settles at a value slightly larger than observed near 1.4 GPa. It should be noted that the broadening at 503 K is much less, changing

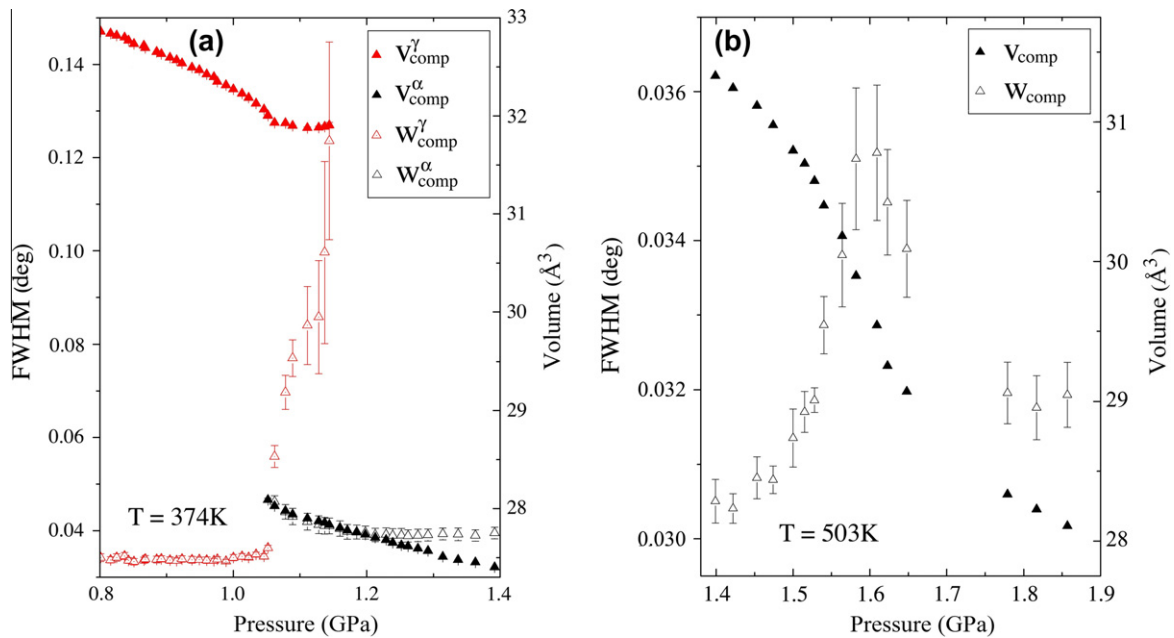


Fig. 5. The FWHM of a [2 2 0] Bragg peak and volume as a function of pressure for two isothermal compressions of polycrystalline Ce metal: (a) $T = 374 \text{ K}$ and (b) $T = 503 \text{ K}$. Examining the EOS for $T = 374 \text{ K}$, which is marked by the solid red and black triangles, the $\gamma \leftrightarrow \alpha$ transformation is apparent. The FWHM of the [2 2 0] diffraction peak for γ increases near the transformation until it disappears with the disappearance of the phase. At $T = 503 \text{ K}$, there is only one fcc phase that continuously changes with pressure. The FWHM of the [2 0 0] diffraction peak also shows a maximum of width, in this case occurring near the inflexion point of EOS. Note that the amount of broadening at 503 K is much less, changing by $\sim 0.006^\circ$, whereas at 374 K the broadening changes by $\sim 0.085^\circ$. (For interpretation of the references to colour in this figure legend, the reader is referred to the web version of this article.)

from 0.03° to 0.036° ($\Delta \sim 0.006$), than at 374 K, where the broadening changes from 0.035° to 0.12° ($\Delta \sim 0.085$).

3.2. Single crystal metal

In this section, we consider results for single-crystal samples, enabling us to examine the $\gamma \leftrightarrow \alpha$ phase transformation in greater detail. Samples were again compressed then slowly released at various temperatures while the crystal structure was monitored via X-ray diffraction.

X-ray diffraction patterns acquired along the $[0\ 0\ 1]$ direction of a single crystal sample are shown for three different pressures in Fig. 6: (a) 0.32 GPa, which is only γ -Ce; (b) 0.61 GPa, which is both α - and γ -Ce; and (c) 1.19 GPa, which is only α -Ce. The diffraction patterns clearly show fourfold symmetry at each pressure. This solidifies our first

important result, namely that the structure remains fcc across the $\gamma \rightarrow \alpha$ transformation. While the polycrystalline diffraction patterns in the inset of Fig. 2 supported this, the single crystal patterns in Fig. 6 finalize the result. The second important result is that the structure retains crystallographic orientation during the $\gamma \rightarrow \alpha$ transformation. This is the first direct evidence that the structure of Ce metal simply reduces the unit cell size of the fcc lattice during the $\gamma \rightarrow \alpha$ transformation, with no change in geometric orientation.

The diffraction peaks in Fig. 6 are streaked azimuthally due to slight lattice misorientation. The angular variation of the $[2\ 0\ 0]$ reflections for γ -Ce is about $7\text{--}8^\circ$. At high pressure, where only α -Ce is present, the streaking is about $10\text{--}11^\circ$. The fact that the streaking increases during the $\gamma \rightarrow \alpha$ transformation suggests that the amount of lattice misorientation increases with the phase transformation.

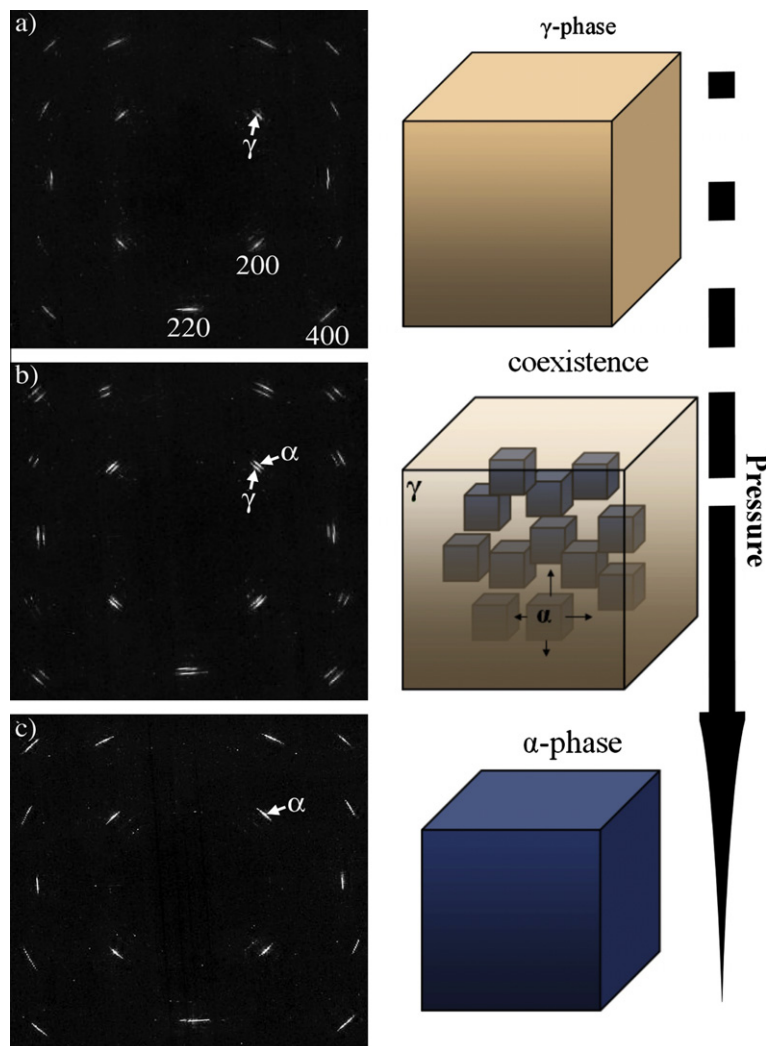


Fig. 6. Synchrotron radiation X-ray diffraction patterns acquired along the $[0\ 0\ 1]$ direction of single crystalline Ce metal at 318 K. Three different pressures are shown on the left: (a) 0.32 GPa (γ -Ce), 0.61 GPa (α - and γ -Ce) and 1.19 GPa (α -Ce). At 0.61 GPa, γ and α coexist, with the same structure and the same orientation but a 14% difference in volume. The diffraction patterns clearly show that the structure retains orientation of the $[0\ 0\ 1]$ direction and the structure simply reduces its lattice size. (Right) A potential transformation mechanism based on our experimental observation: as the γ sample is compressed, numerous small blocks of α -phase nucleate and grow uniformly across the sample. This is supported by diffraction data that consistently show a mixture of both phases when the $20\ \mu\text{m}$ beam was scanned across the sample (diameter $\sim 100\ \mu\text{m}$). As the particles grow and impinge upon one another, their interfaces are in registry, allowing the α crystallites to unite to form one large crystal.

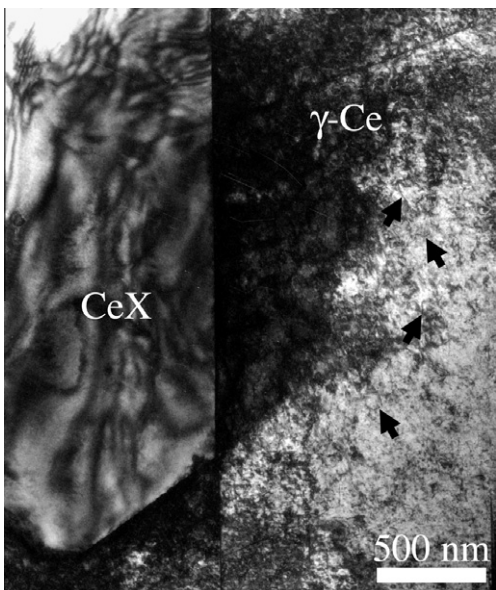


Fig. 7. Bright-field TEM image of an impurity particle in Ce metal. Besides the bend and thickness contours, which are the blurry black lines in each phase, the metal is much more mottled due to defects (and some surface oxide). These defects were always present in our investigations, even after annealing for several days in a vacuum furnace at 800–900 K.

Lattice misorientation and damage are not only generated during the transformation, but also occur intrinsically within the metal. This is illustrated in the bright-field TEM image in Fig. 7, which shows a two-phase mixture of γ -Ce and an impurity particle. The particle is labeled CeX, since it was not investigated to delineate the phase, but is likely CeH_2 . When rare earth and actinide metals are ion milled to electron transparency, as was done with this sample, hydride particles often form as an unwanted secondary phase [33,37]. The exact composition is not crucial in the present purpose, but simply the fact that the impurity phase makes a strong contrast with the metal. The defect-free particle is uniform in intensity other than dark curves due to bending and thickness changes that influence electron scattering. On the other hand, the γ -Ce region shows a crystal with damage, such as dislocations, which are the dark lines marked by arrows in Fig. 7.¹ Dislocations will cause diffraction peaks to blur rather than streak, but the point remains: damage is always present in Ce metal, even after annealing for several days in a vacuum furnace at 800–900 K. Whether annealing for weeks or months would remove this lattice damage was not tested. However, our investigations have clearly shown that Ce metal retains a large amount of intrinsic damage and lattice misalignment, similar to Pu [38].

The EOS of single crystal was determined at several temperatures using X-ray diffraction in the same manner as for the polycrystalline samples. The data are shown in Fig. 8,

¹ There are also intensity contributions in γ -Ce due to oxide on the two surfaces of the TEM sample; however, this can be examined separately from the damage within the metal.

where (a) is for 340 K and (b) is for 388 K. Both plots show the EOS of γ and α during compression and decompression using the same markers as for Fig. 3a and b. The overall behavior is similar to that of the polycrystalline samples, exhibiting hysteresis and a pressure region with a mixture of γ and α . However, the EOS in Fig. 8a does not show an increase in the volume of γ during compression once the α phase begins to form. Rather, once α forms, the volume of γ continues to decrease, though at a slower rate than before α appeared. During decompression, α appears to reduce volume when γ forms; however, given the error, this is not clear. Certainly the level of backtracking of the lattice volume with pressure observed for single crystals is less than that observed for the polycrystalline samples, such as that in Fig. 3a. This suggests that grain boundaries play a role in the phase transformation, altering the results between single and polycrystals.

The FWHM of the [2 2 0] reflection and the volume of a single crystal were examined during the $\gamma \leftrightarrow \alpha$ phase transformation for an isothermal compression at 388 K. The EOS results in Fig. 9 are similar to that obtained during isothermal compression at 374 K for the polycrystalline sample shown in Fig. 5a. However, while the form of the FWHM results are similar, the magnitude is much smaller. The width at 388 K for the single crystal changes from 0.033° to 0.065° ($\Delta \sim 0.032$), whereas the width at 374 K for the polycrystal changes from 0.035° to 0.12° ($\Delta \sim 0.085$). The larger broadening of diffraction peaks in polycrystalline sample suggests that the grain boundary network influences the lattice, possibly creating more damage through increased strain during the transformation.

4. Discussion

Now that we have established that the $\gamma \leftrightarrow \alpha$ phase transformation remains in crystallographic orientation and is isostructural with both phases being fcc, we can examine what this means for the transformation as well as the γ - α interface.

4.1. The $\gamma \leftrightarrow \alpha$ transformation

The [0 0 1] X-ray diffraction patterns of single crystalline Ce metal at 318 K in Fig. 6 show a coexistence of γ and α at 0.61 GPa. Both phases are fcc with the same orientation, but have a 14% volume difference at this temperature. The diffraction patterns clearly show that the fcc structure retains orientation during the $\gamma \rightarrow \alpha$ transformation, where the structure simply reduces the unit cell size. Ultrasonic measurements of Ce at high pressure demonstrate that the $\gamma \rightarrow \alpha$ transformation is due to a softening of the compressional mode, whereas the shear mode increases with pressure, which is in agreement with the structure retaining symmetry [39]. Given this information, the next logical question is what is the transformation mechanism?

Based on our experimental observation, a potential transformation mechanism is through a large number of

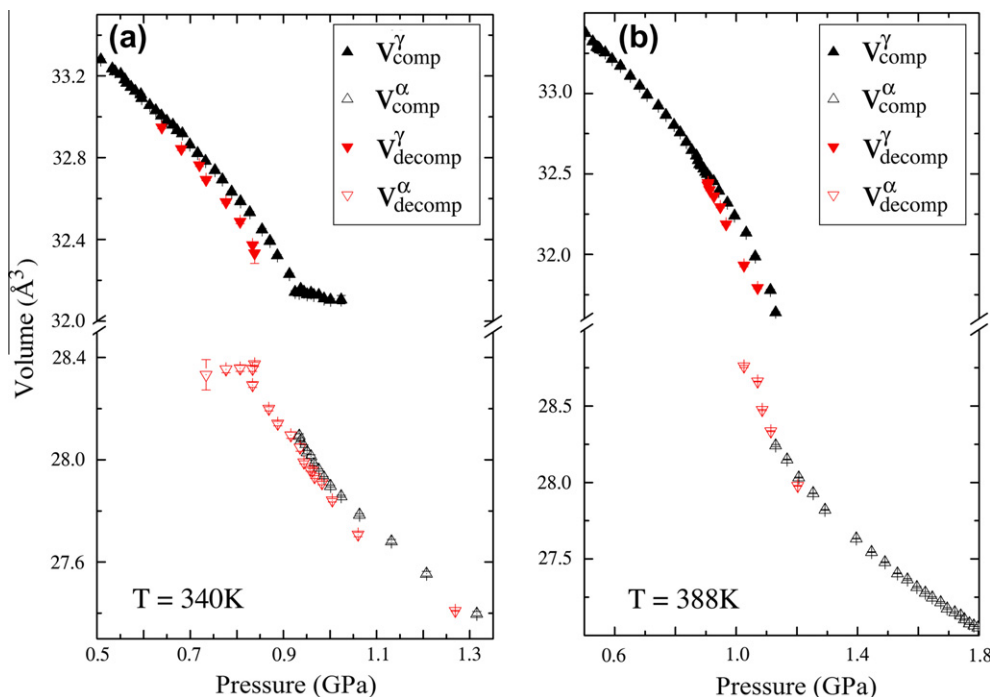


Fig. 8. Two pressure–volume plots showing the EOS of single crystalline Ce metal: (a) $T = 340$ K and (b) $T = 388$ K. The EOS are similar to the results for polycrystalline metal in Fig. 3.

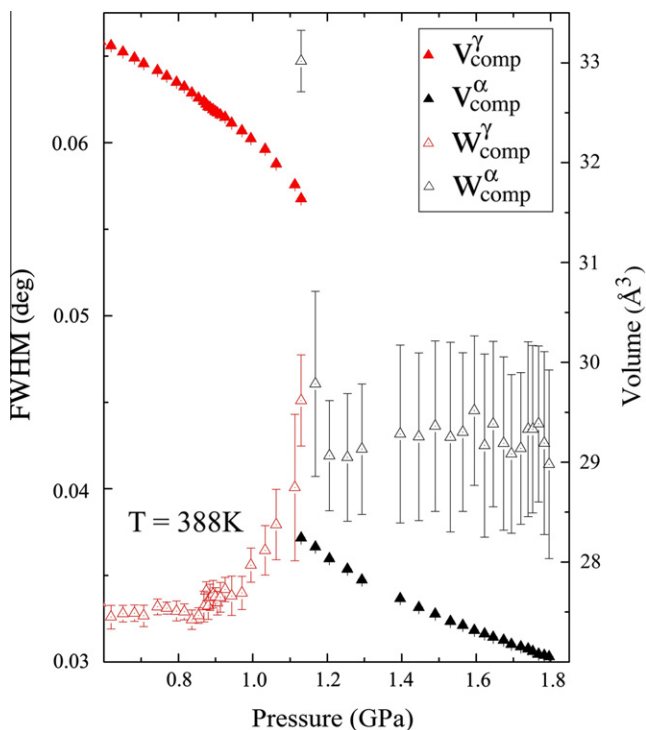


Fig. 9. The FWHM of the [2 2 0] Bragg peak and volume as a function of pressure for isothermal compression of single crystalline Ce metal at $T = 388$ K.

uniformly distributed precipitates. During the $\gamma \rightarrow \alpha$ transformation upon compression, numerous small precipitates of the α -phase would nucleate in the γ crystal and grow

with increased pressure. This is supported by the diffraction data near 0.61 GPa, which consistently show a mixture of both phases when the $20 \mu\text{m}$ beam was scanned across the $\sim 100 \mu\text{m}$ sample. Had there been large regions of α that nucleated, grew and consumed the γ -crystal, the pattern would change with beam location. However, this was not the case. Therefore, a single crystal of γ transforms to a single crystal of α during the $\gamma \rightarrow \alpha$ transformation even though the process is achieved through the nucleation and growth of many sites. This is possible because each α precipitate is in crystallographic orientation with the γ lattice. As the particles grow and impinge upon one another, their interfaces are in registry, allowing the α precipitates to unite and form one large crystal. The result is a single crystal of α (upon compression) or γ (upon release) once the transformation is complete.

The transformation is reversible, although it becomes more retarded with each cycle due to increasing lattice misorientation and damage. This was shown by Zukas et al. [27], who examined the $\gamma \rightarrow \alpha$ transformation using hydrostatic compression in a Harwood press with argon as the pressure medium, simultaneously monitoring pressure, temperature and specimen length. When completely transformed to α through compression then returned to γ on release, the original grains were permanently deformed, exhibiting deformation bands near (1 1 1) planes with some curvature. Optical micrographs of the sample before and after compression revealed a microstructure that was similar, but with large amounts of plastic deformation. They also performed dilatometry traces of a sample through five compression–release cycles and found the per-

cent transformed reduced with each cycle. This supports the hypothesis that growing damage from each compression cycle begins to impede the transformation. Indeed, accumulation of lattice damage has been found to inhibit transformation in other large-volume transformations, such as the $\delta \rightarrow \alpha$ transformation in Pu–Ga [40]. Finally, Zukas et al.'s results showed that γ grains exhibited a lattice misorientation of slightly more than 2° before the $\gamma \rightarrow \alpha$ transformation, but after the transformation and return to the γ phase at room pressure, the misorientation increased to about 10° . This is in agreement with the general trend of increasing lattice misorientation between γ and α shown in Fig. 6.

Bustingorry et al. [41] used a non-linear elastic model to explain the thermodynamics of the volume collapse in cerium. Their model reproduces the volume hysteresis observed in our pressure experiment, and a negative bulk modulus. Their model also shows that the width of the hysteresis loop shrinks with increasing temperature, terminating at a critical point. The shortcoming of their model, however, is in the assumptions. First, they consider the α and γ phases to be elastically isotropic with the same value of the elastic coefficients. This is surely not the case. Second, their model is fully coherent, i.e. with no structural defects during the transformation. This too is clearly incorrect. The proof is given by the deformation bands observed by Zukas et al. [27] after repeated cycling of the $\gamma \leftrightarrow \alpha$ transformation. Regardless of these shortcomings, which the authors freely point out themselves, the model agrees with many of the features of the Ce metal phase diagram.

4.2. The γ – α interface

Our pressure–temperature diffraction results, combined with the clear evidence of deformation bands by Zukas et al. [27], allow us to formulate a model for the γ – α interface that includes misfit edge dislocations.

Deformation bands can be explained as a result of localized lattice rotations, where bending of crystal planes occurs due to accumulation of a large number of edge dislocations with the same sign [42]. Such a dislocation structure is a natural consequence of the lattice mismatch at the γ – α interface and the identical crystallographic orientation between phases. This is illustrated in Fig. 10, which is an atomic model showing an (001) interface between two cubic crystals with a large volume difference. A periodic array of edge dislocations (red T marks) with the same sign decorate the γ – α interface in Fig. 10, since their presence is necessary to accommodate the lattice mismatch. During the $\gamma \rightarrow \alpha$ transformation, there is a $\sim 17\%$ volume change between two phases that have the same structure and orientation. This corresponds to a roughly 5% change in linear dimension, or one dislocation per 20 atoms along the (001) interface required to accommodate the misfit between γ - and α -Ce. We assume an (001) interface in Fig. 10, but the same argument applies for an interface on any crystallographic plane, since γ and α are in the same

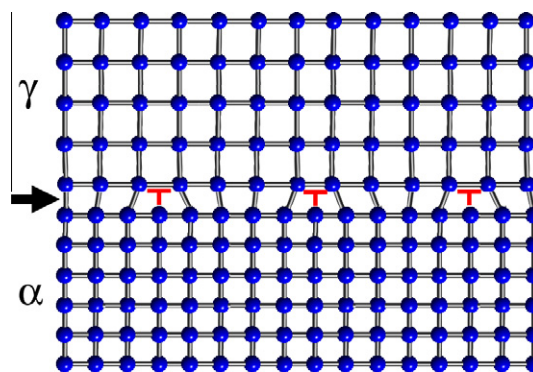


Fig. 10. Atomic model showing an (001) interface between two cubic crystals with a large volume difference. The arrow indicates the planar interface and the three red T marks indicate edge dislocations that form a periodic array along the interface. A periodic array of misfit edge dislocation is necessary to accommodate the large volume difference at the γ – α interface. This could act as a source of the edge dislocations needed to produce the deformation bands observed by Zukas et al. [27]. (For interpretation of the references to colour in this figure legend, the reader is referred to the web version of this article.)

crystallographic orientation. The interface could even be composed of terraces, ledges and kinks, as has often been observed [43,44].

The dislocation structure in the mixed phase system, required by the identical crystallographic registries, translates directly to the post-transformation system. Consider a compression transformation ($\gamma \rightarrow \alpha$), with particles α_1 and α_2 separated by region γ , which is schematically drawn as “coexistence” in Fig. 6b. The dislocations on the α_1 – γ interface will be of opposite sign to the dislocation on the α_2 – γ interface that faces the α_1 particle. As particles α_1 and α_2 impinge upon each other, the dislocations should annihilate. However, the dislocation positions at each α – γ interface will be incommensurate, meaning not all dislocations will annihilate. Put simply, large-scale dislocation alignment would not be possible. Each time the $\gamma \leftrightarrow \alpha$ transformation occurs with a cycle in pressure, more dislocations remain, accumulating to produce deformation bands near (111) planes and to retard the transformation.

The exact nature of the α – γ interface must be examined using high-resolution and weak-beam TEM on a partially transformed Ce sample. We attempted the $\gamma \rightarrow \alpha$ transformation in a transmission electron microscope using a liquid He holder that achieved 8 K. The sample jumped during heating and cooling, suggesting that the transformation occurred in the thicker part of the sample; however, no change was observed in the areas thin enough for electron transparency. The holder remained cold for ~ 45 min, which might have been too short a period for the thin portions of the foil to transform. Using a transmission electron microscope with dedicated liquid He cooling, where the sample can be left for days in the alpha phase field, may be the key to achieving transformation to α in the transmission electron microscope.

5. Summary

Using X-ray diffraction measurements at high pressure and high temperature, we examined the $\gamma \leftrightarrow \alpha$ transformation in poly- and single-crystalline samples of Ce. This was achieved through successive compression and decompression cycles in a DAC at temperatures below and above the critical point. Our results show that the crystal structure remains fcc for both the γ and α phases. The results also show that the fcc structure stays in crystallographic orientation, simply reducing in size during the transformation. Upon transformation to α in single crystals, increased diffraction streaking is observed due to growing lattice misorientation and damage. Using a simple atomic lattice model, we argue that a periodic array of misfit edge dislocations is necessary to accommodate the large volume difference at the γ – α interface. These could act as a source of the edge dislocations needed to produce the deformation bands near (1 1 1) observed Zukas et al. [27].

Acknowledgements

Lawrence Livermore National Laboratory is operated by Lawrence Livermore National Security, LLC, for the US Department of Energy, National Nuclear Security Administration under Contract DE-AC52-07NA27344. This work was supported by an ANR contract (No. ANR-08-BLAN-0109-01). We thank D. Antonangeli, B. Amadon and C. Denoual for fruitful discussion and M. Hanfland at ESRF for his help with the experiments.

References

- [1] McHargue CJ, Yakel Jr HL. *Acta Metall* 1960;8:637.
- [2] Rashid MS, Altstetter CJ. *Trans Metall Soc AIME* 1966;236:1649.
- [3] Lipp MJ, Jackson D, Cynn H, Aracne C, Evans WJ, McMahan AK. *Phys Rev Lett* 2008;101:165703.
- [4] Lawson AW, Tang TY. *Phys Rev* 1949;76:301.
- [5] Johansson B. *Philos Mag* 1974;30:469.
- [6] Allen JW, Martin RM. *Phys Rev Lett* 1982;49:1106.
- [7] Gustafson DR, McNutt JD, Roellig LO. *Phys Rev* 1969;183:435.
- [8] Kornstädt U, Lässer R, Lengeler B. *Phys Rev B* 1980;21:1898.
- [9] Lengeler B, Materlik G, Müller JE. *Phys Rev B* 1983;28:2276.
- [10] Allen GC, Trickle IR, Tucker PM. *Philos Mag B* 1981;43:689.
- [11] Murani AP, Levett SJ, Taylor JW. *Phys Rev Lett* 2005;95:256403.
- [12] Manley ME, McQueeney RJ, Fultz B, Swan-Wood T, Delaire O, Goremychkin EA, et al. *Phys Rev B* 2003;67:014103.
- [13] Haule K, Oudovenko V, Savrasov SY, Kotliar G. *Phys Rev Lett* 2005;94:036401.
- [14] van der Eb JW, Eb AB, Kuz'menko, van der Marel D. *Phys Rev Lett* 2001;86:3407.
- [15] Held Y, McMahan AK, Scalettar RT. *Phys Rev Lett* 2001;87:276404. *Phys Rev B* 2003;67:075108.
- [16] Moore KT, van der Laan G. *Rev Mod Phys* 2009;81:235.
- [17] Rueff J-P, Hague CF, Mariot J-M, Journal L, Delaunay R, Kappler J-P, et al. *Phys Rev Lett* 2004;93:067402.
- [18] Dallera C, Grioni M, Palenzona A, Taguchi M, Annese E, Ghiringhelli G, et al. *Phys Rev B* 2004;70:085112.
- [19] Eliashberg G, Capellmann H. *JETP Lett* 1998;67:125.
- [20] Davis BL, Adams LH. *J Phys Chem Solids* 1964;25:379.
- [21] Nikolaev AV, Michel KH. *Phys Rev B* 2002;66:054103.
- [22] Tsvyashchenko AV, Nikolaev AV, Velichkov AI, Salamatin AV, Fomicheva LN, Rysny GK, et al. *Phys Rev B* 2010;82:092102.
- [23] Porsch F, Holzapfel WB. *Phys Rev Lett* 1993;70:4087.
- [24] Zhao YC, Porsch F, Holzapfel WB. *Phys Rev B* 1995;52:134.
- [25] Lashley JC, Lawson AC, Cooley JC, Mihaila B, Opeil CP, Pham L, et al. *Phys Rev Lett* 2006;97:235701.
- [26] Moore KT, Söderlind P, Schwartz AJ, Laughlin DE. *Phys Rev Lett* 2006;96:206402.
- [27] Zukas EG, Pereyra RA, Willis JO. *Metal Trans A* 1987;18:35.
- [28] Decremps F, Belhadi L, Farber DL, Moore KT, Occelli F, Gauthier M, et al. *Phys Rev Lett* 2011;106:065701.
- [29] Stassis C, Gould T, McMasters OD, Gschneidner Jr KA, Nicklow RM. *Phys Rev B* 1979;19:5746.
- [30] Stassis C, Loong C-K, McMasters OD, Nicklow RM. *Phys Rev B* 1982;25:6485.
- [31] Farber DL, Antonangeli D, Aracne CM, Benterou J. *High Press Res* 2006;26:1.
- [32] Moore KT, Chung BW, Morton SA, Schwartz AJ, Tobin JG, Lazar S, et al. *Phys Rev B* 2004;69:193104.
- [33] Moore KT, Wall MA, Schwartz AJ, Chung BW, Morton SA, Tobin JG, et al. *Philos Mag* 2004;84:1039.
- [34] Cahn JW. *Acta Metal* 1961;9:795.
- [35] Soffa WA, Laughlin DE. In: Aaronson HI, Laughlin DE, Sekerka RF, Wayman CM, editors. *Solid–solid phase transformations, proceedings of an international conference*, Warrendale, PA: AIME; 1982. p. 159.
- [36] Moore KT, Johnson WC, Howe JM, Aaronson HI, Veblen DR. *Acta Mater* 2002;50:943–56.
- [37] Moore KT. *Micron* 2010;41:336.
- [38] Moore KT, Krenn CR, Wall MA, Schwartz AJ. *Metal Mater Trans A* 2007;38:212; Schwartz AJ, Cynn H, Blobaum KJM, Wall MA, Moore KT, Evans WJ, et al. *Prog Mat Sci* 2009;54:909.
- [39] Decremps F, Antonangeli D, Amadon B, Schmerber G. *Phys Rev B* 2009;80:132103.
- [40] Hecker SS, Harbur DR, Zocco TG. *Prog Mater Sci* 2004;49:429.
- [41] Bustingorry S, Jagla EA, Lorenzana J. *Acta Mater* 2005;53:5183.
- [42] Hill RE, Abbaschian R. *Physical metallurgy principles*. 3rd ed. Boston: PWS Publishing; 1992.
- [43] Enomoto M, Furuhashi T. *J Iron Steel Inst Jpn* 1991;77:735.
- [44] Kamat SV, Hirth JP. *Acta Metal Mater* 1994;42:3772.